Chemical Engineering Journal 109 (2005) 97–106

Chemical Engineering Journal

www.elsevier.com/locate/cej

Scale-up effect of riser reactors (3) axial and radial solids flux distribution and flow development

Aijie Yan, Jeff Ball, Jesse (Jingxu) Zhu *

Department of Chemical and Biochemical Engineering, University of Western Ontario, 1151 Richmond Street, London, Ont., Canada N6A 5B9

Received 18 August 2004; received in revised form 30 March 2005; accepted 31 March 2005

Abstract

The influence of riser diameter on the axial and radial solids flux and flow development is studied in three riser circulating fluidized bed reactors of different diameters (76, 100 and 203 mm i.d. risers). A suction probe was used for the direct measurement, while the calculated local solids flux data obtained from solids velocity and concentration measured by two separate fibre optic probes were used to compare. Two shapes were found for the radial profile of the solids flux, a parabolic shape and a flat core shape. The shapes obtained could be predicted, based on the operating conditions, using a new concept of the effective solids saturation carrying capacity. The radial profile of solids flux is less uniform in a larger riser than in a smaller riser. Flow development is slower with the increase of riser diameter. The operating conditions were found to affect the solids flux in each reactor in the same general fashion: increasing gas velocity decreased the amount of downflow solids in the risers; increases in the solids circulation rate caused more solids to flow downwards.
© 2005 Elsevier B.V. All rights reserved.

Keywords: Scale-up; Hydrodynamics; Fluidization; Powder technology; Flow development; Solids flux

1. Introduction

Circulating fluidized bed (CFB) riser reactors were first developed in the 1940s as an improvement on the fixed bed processes used in the petroleum industry to crack hydrocarbons [1]. The higher gas velocities lead to better contact between the phases, which improved the reaction rates and increased productivity rates. For other technical reasons, however, turbulent fluidized beds were used first to replace the fixed bed reactors until the late 1960s when the riser started to become the standard reactor in cracking processes. The CFB reactor has also seen application in combustion operations. Due to its increasing importance, the CFB riser reactor has been the subject of many studies [2–6].

The solids flux is a key parameter in the study of the hydrodynamics in CFBs. The solids flux is defined as a mass flowrate through a unit area. The distribution of the solids across the column radius is of importance in the successful design of riser reactors. The location of the solids can affect the reaction rates, erosion and the heat transfer within the riser reactor. Due to its importance, the solids flux has been the subject of a number of studies as reported in the literature [7–23]. The researchers have studied such effects as the operating conditions and the axial, radial and angular positions.

The shape of the radial solids flux profile has been reported in the literature by many different researchers [7–9,11,16–21,23]. Though there exist many reports on the shapes of the solids flux profiles, no general consensus has been reached. The first belief was that the shape of the radial solids flux profiles was parabolic [7,8,11]. However, recently reported results indicate that the shape of the radial solids flux profile was much flatter [9,16,17,19,20]. The shapes of the profiles tend to depend on the operating conditions. High values of G_s or low values of U_g appears to favor the parabolic shape, whereas lower G_s or high U_g make the shapes of the profile much more flat. A regime of similar radial profiles of reduced solids flux (local solids flux divided by the cross-sectional mean solids flux) was reported to exist in risers [7,12]. When comparing the reduced radial profiles of solids

* Corresponding author. Tel.: +1 519 661 3807; fax: +1 519 850 2441.
E-mail address: jzhu@uwo.ca (J. Zhu).

1385-8947/$ – see front matter © 2005 Elsevier B.V. All rights reserved.
doi:10.1016/j.cej.2005.03.017

Nomenclature

G_s	overall solids circulating rate (kg/m^2 s)
G_{sL}	local solids flux (kg/m^2 s)
G_s^*	solids saturation carrying capacity (kg/m^2 s)
H	distance from the riser distributor (m)
r/R	reduced radial position
U_g	superficial gas velocity (m/s)
U_{suc}	suction velocity (m/s)

flux, under the same gross solids flux (=solids circulation rate), the researchers reported that these profiles were of the same shape and magnitude regardless of the other operating condition used.

In addition, these studies were conducted only at limited locations and no comprehensive study has been reported for the complete measurements of the axial and radial profiles of local solids flux in both upflow and downflow directions in an entire riser. Previous studies were mostly limited to lower flux conditions ($G_s < 100$ kg/m^2 s) and columns of shorter lengths (5–7 m). Furthermore, the column diameter is a parameter that has not been the subject of a systematic study, since very few fluidization laboratories posses more than one riser. Only a rough description of scale-up effect was given in [22], by comparing the data from Harris [24] and Werdermann [25]. It is therefore necessary to carry out systematic new tests under high solids fluxes within longer risers of different diameters. This paper will present results obtained in three long risers of different diameters capable of attaining solids fluxes over 200 kg/m^2 s.

2. Experimental apparatus

The tests were conducted in three risers of 76 mm (3 in.), 100 mm (4 in.) and 203 mm (8 in.) inner diameter. The 100 mm diameter riser was 15.1 m long and the 76 mm and 203 mm risers were 10 m long. The solids used in three columns were FCC particles and had a particle diameter of 67 μm and a density of 1500 kg/m^3. The gas in these experiments was air at ambient conditions.

The 100 mm column is shown in Fig. 1. The solids start off in the storage tank and a butterfly valve is used to control the flow of the solids into the riser. The solids flow from the storage tank into the riser distributor region where the solids are fluidized by the auxiliary air. The main riser air enters through a series of thirty-seven 13 mm o.d. tubes extending 0.30 m into the riser bottom to carry the gas–solids suspension up the riser and through a smooth exit into the primary cyclone. The bottom of this cyclone connects to the distributor of the downer. The riser air from the cyclone is sent through a pair of secondary and tertiary cyclones and a bag filter for further cleaning before being exhausted to the atmosphere. From the downer distributor, the gas–solids suspension travels along the downer to the exit where the solids are separated using a fast inertial separator. The gas is then sent through a secondary and a tertiary cyclone and a bag filter for final cleaning. The downer and riser gas flow rates can be set independently from each other. The solids from the fast separator are then returned to the storage tank during normal operation. The diverting valve is used to measure G_s, when the flow of solids is switched into the measuring tank for a known amount of time. Measuring the height of the accumulated solids allows G_s to be determined.

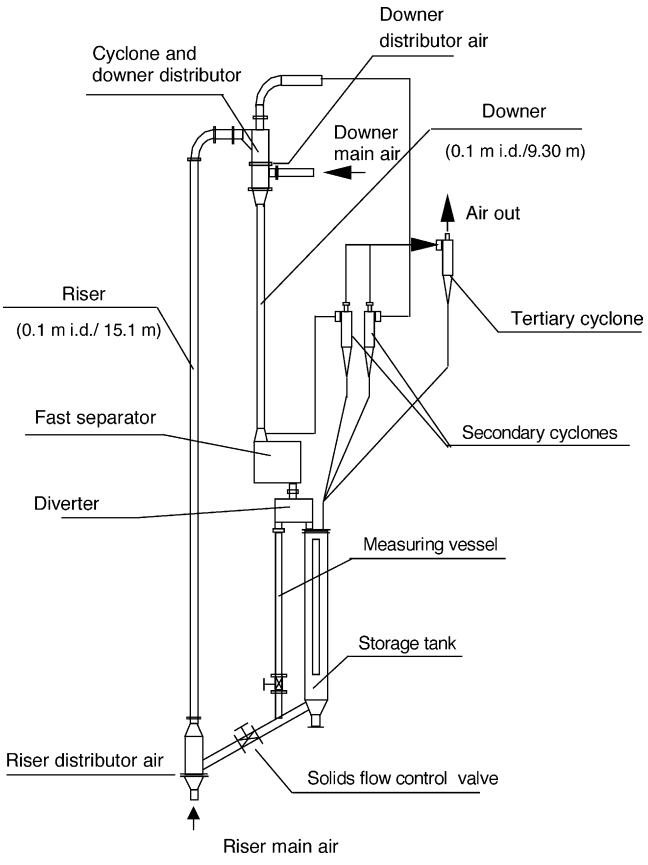

Fig. 1. Schematic of the 100 mm i.d. riser/downer apparatus.

In a twin riser apparatus, the 76 mm riser is paired with a 203 mm diameter riser of the same length (10 m), as shown in Fig. 2. The solids start in the storage tank and flow into the risers. The flow of solids is controlled using two separate butterfly valves for the two risers. The configurations of these twin risers are exactly the same except for the diameter. Only one riser is operated at a certain time. Each riser distributor was a perforated plate. The gas–solids mixture travels up the riser and is separated using a series of three cyclones. The solids are returned to the storage tank and the gas is further cleaned using a bag filter. At the top of the storage tank, a section of the column with two half valves at each end is used to measure G_s. This measuring section is a cylinder with a partition down the middle. When G_s is being measured, the upper valve diverts the solids flow down half of the cylinder, the bottom of which is sealed by the lower valve. The height of

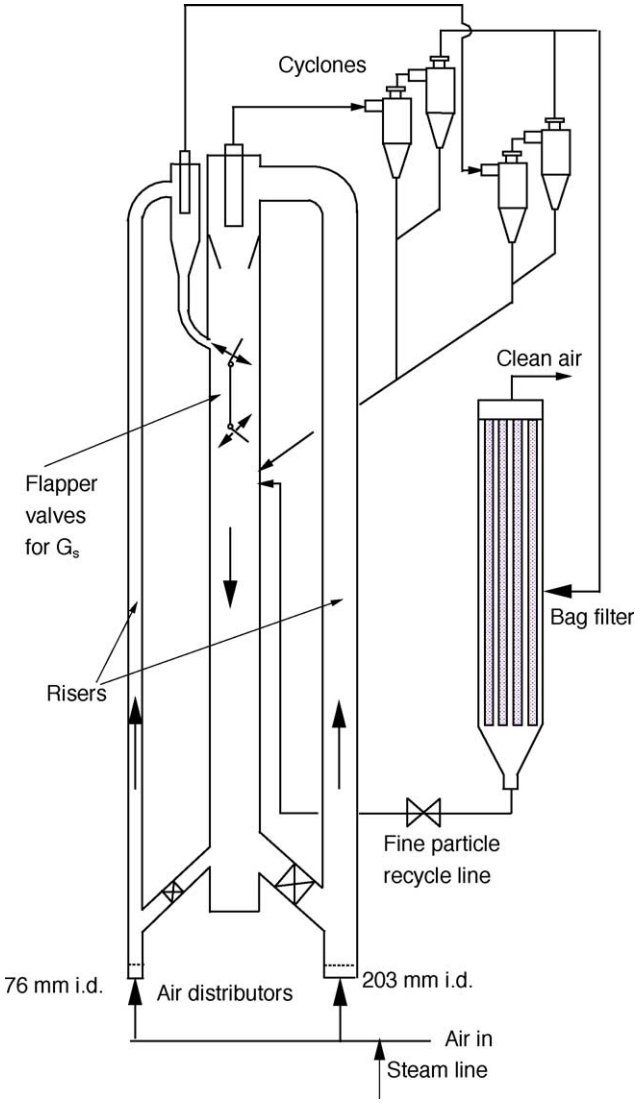

Fig. 2. Schematic of the twin riser system.

the accumulated solids is measured for a known time, which allows G_s to be determined.

For the measurement of local solids fluxes, if a sample is taken at suction velocity equal to local instantaneous gas velocity, it is called isokinetic sampling; otherwise, it is called non-isokinetic sampling. Isokinetic sampling will require the use of more auxiliary equipment and constant variations of the suction velocity, whereas non-isokinetic sampling requires less auxiliary equipment.

The solids fluxes for these tests were measured using a non-isokinetic suction probe. The probe used suction to sample solids for a set amount of time. From the mass of solids collected, the local solids flux, G_{sL}, was calculated. Due to the nature of the flow in the riser, a C-shaped probe tip was constructed. This permitted the sampling of the upflow and downflow of solids at the same axial and radial position by turning the probe 180° on its axis. A schematic diagram of the probe tip is shown in Fig. 3.

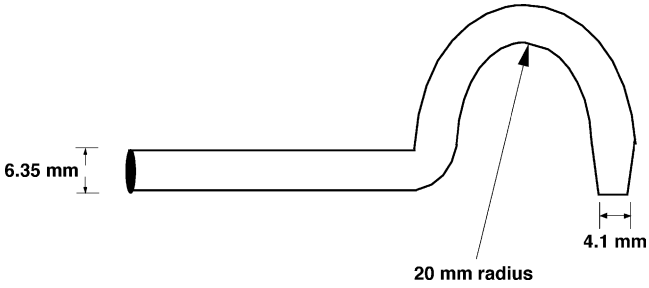

Fig. 3. Schematic of probe tip used in the risers.

When suction is used, it is important to determine the effects, if any, of the suction velocity on the mass of solids collected. When no effect was seen, this permitted the use of non-isokinetic sampling, which requires less auxiliary equipment and is much easier to use than isokinetic sampling. A comprehensive set of tests was completed in the 100 mm riser, with six samples withdrawn at each radial position for four different U_{suc} at $U_g = 5.5$ m/s and $G_s = 100$ kg/m^2 s. The average results of these tests are presented in Fig. 4, which includes the values of the upflow, downflow and net solids flux. The figure shows that little effects on G_{sL} were present when U_{suc} was varied around U_g, at the radial positions tested for the upflowing solids. This was also the case for the downflowing solids. These initial tests further showed that solids only significantly flow downwards extremely close to the riser wall. Fig. 4b is at $r/R = 0.81$ and there are no significant downflowing solids at this point fairly close to the wall, as compared with Fig. 4a which is at $r/R = 0.98$ where a significant amount of solids are flowing downwards. As would be expected the mean G_{sL} was not greatly affected by changes in U_{suc}, since the mean G_{sL} is equal to the up G_{sL} minus down G_{sL}. Due to the lack of dependence of solids fluxes on U_{suc}, it was therefore possible to use non-isokinetic sampling for the experiments. During the experiments, U_{suc} was set at U_g for upwards solids flux and at a very small velocity (near-zero condition) for downwards flux.

In these three risers, solids flux was measured at 11 radial positions ($r/R = 0.00$, 0.16, 0.38, 0.50, 0.59, 0.67, 0.74, 0.81, 0.87, 0.92 and 0.98). To ensure accuracy, six samples were taken at each radial position in these three columns. In the twin riser system, tests were taken at four heights ($H = 1.52$, 3.96, 6.30 and 8.74 m in the 76 mm riser and $H = 1.47$, 3.91, 5.84 and 8.79 m in the 203 mm riser). In the 100 mm riser, measurements were completed at six different axial positions ($H = 0.97$, 2.70, 4.53, 6.30, 10.14 and 13.67 m). The operating conditions for three risers are given in Table 1.

3. Results and discussion

3.1. Shape of radial profiles of solids flux

Fig. 5 presents a comprehensive report of the components of the local solids flux, G_{sL} (upflow, downflow, net), at the top

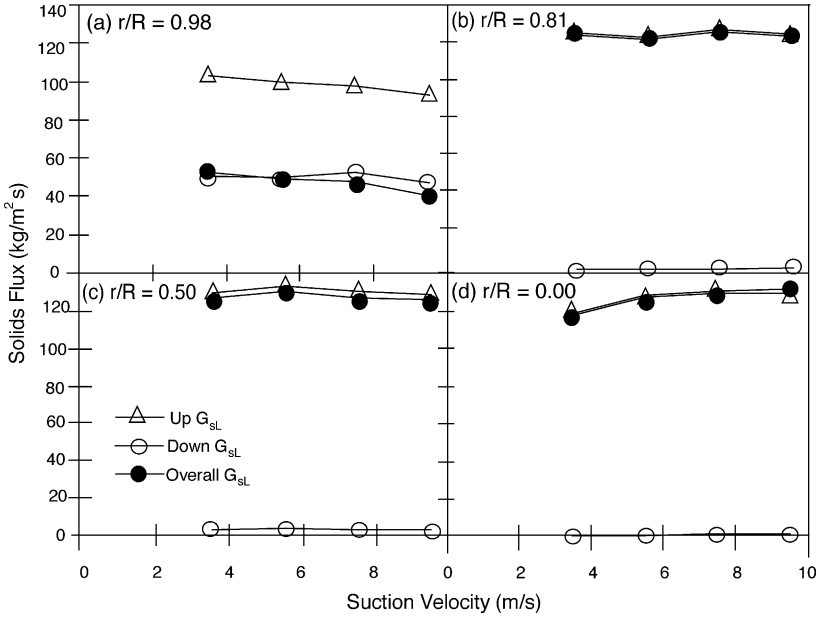

Fig. 4. Effects of suction velocity on the solids fluxes at various radial positions in the riser (U_g = 5.5 m/s, G_s = 100 kg/m^2 s).

measurement (H = 8.74 m) level in the fully developed region in the 76 mm riser. Fig. 5a presents the results for the upflowing solids flux in the riser and show that the shapes of radial profiles are rather flat, but tend to peak near the wall. Fig. 5b shows the radial profiles for the downflowing solids flux. It is interesting to note that in the central regions of the riser, there are virtually no downflowing solids. Solids do not begin to flow downwards until positions very close to the wall in the fully developed region. The amount of downflowing solids increases to a maximum value at the wall. The upflow and downflow are combined to determine the net solids flux (upflow − downflow = net). The radial profiles of the net solids flux are very flat across the central regions of the riser with a slight peak near the wall. The small peak near the wall is due to the very high solids holdup there.

Fig. 5 can also be used to determine the effects of the operating conditions on the shape of the solids flux profiles in the fully developed region of the 76 mm riser. Fig. 5a shows that G_s had a larger effect than U_g on the upflowing solids flux. Increases in G_s lead to increases in the upflowing G_{sL} at every radial position. This was true at every axial position tested in the riser. On the other hand, U_g had little effect on the upflowing solids flux, as expected. Fig. 5b presents data of the downflowing solids fluxes in the riser. At a constant U_g (=5.5 m/s), increasing G_s from 50 to 100 kg/m^2 and then to 200 kg/m^2 s caused an increase in the downflowing solids at the wall. The increase in the amount of downflowing solids at the wall is much more significant when G_s was increased from 100 to 200 kg/m^2 s than from 50 to 100 kg/m^2 s. Increases in U_g affected the downflowing solids flux to a larger extent than the upflowing solids. Increasing U_g at a constant G_s reduced the amount of downflowing solids at the wall. This was expected as increased U_g increases the potential for the gas to carry more solids upwards, so that the amount of downflowing solids is reduced. The mean solids flux was also affected by the operating conditions, but due to the small amount of downflowing solids, the profiles are affected in the same manner as the upwards flowing solids. Increases in G_s causes increases in G_{sL} at every radial position. Increasing U_g reduces the amount of downflowing solids, so one would expect to see an increase in the mean solids flux. This was, however, not observed because the amount of downflowing solids was rather small and located at limited radial positions so this did not translate into a large effect on the mean G_s.

The radial solids flux profiles shown in Fig. 5 in the fully developed region are similar to the rather flat shape

Table 1
Operating conditions

3 in. riser (0.076 m i.d.) and 4 in. riser (0.100 m i.d.)		8 in. riser (0.203 m i.d.)	
Gas velocity U_g (m/s)	Solids circulation rate G_s (kg/m^2 s)	Gas velocity U_g (m/s)	Solids circulation rate G_s (kg/m^2 s)
5.5	50	5.5	50
3.5	100	5.5	75
5.5	100	5.5	100
8.0	100	8.0	100
5.5	200		

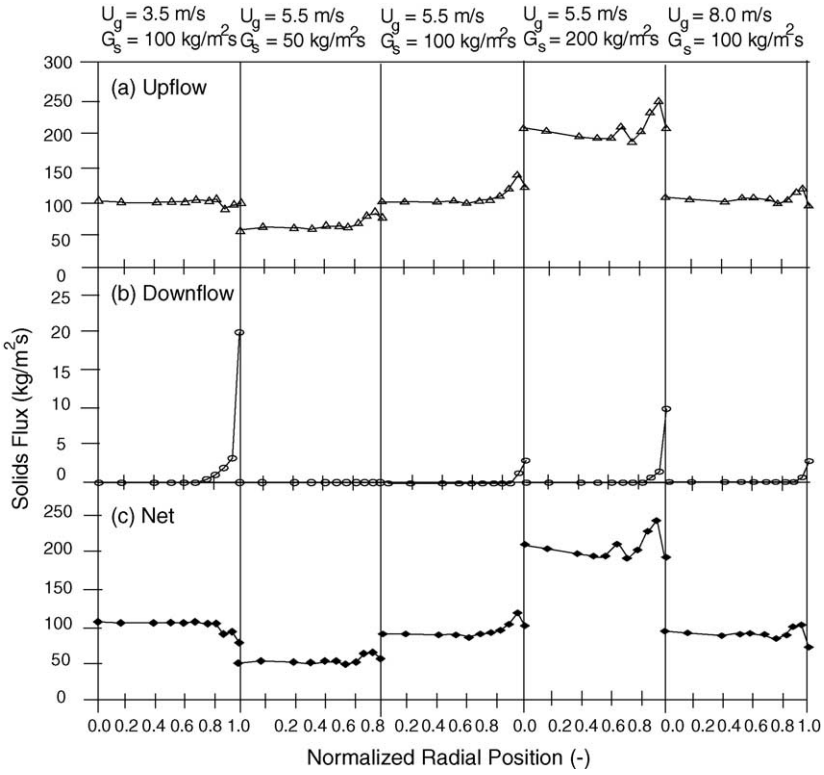

Fig. 5. Effects of operating conditions on the radial profiles of solids flux in the fully developed region (H = 8.74 m) in the 76 mm riser.

reported by some researchers [9,16,17,19], but do not follow the parabolic shape as reported by some other researchers [7,8,11]. As reviewed earlier, there are generally two different types of radial solids flux distributions, the parabola and the flat core with decreasing value towards the wall.

Carefully examining the results from our experiments and those from the literature, it appears that operating conditions with higher solids/gas loading have more tendency to result in the parabolic shape, while experiments under lower G_s but higher U_g tend to produce the more flat radial profile. To further illustrate this, the operating conditions (G_s and U_g) of our experiments and those from the previous studies on radial solids flux distribution are plotted in Fig. 6. In this figure, the solids saturation carrying capacity, G_s^*, calculated from the equation of Bai and Kato [26], is also plotted. The filled sym-

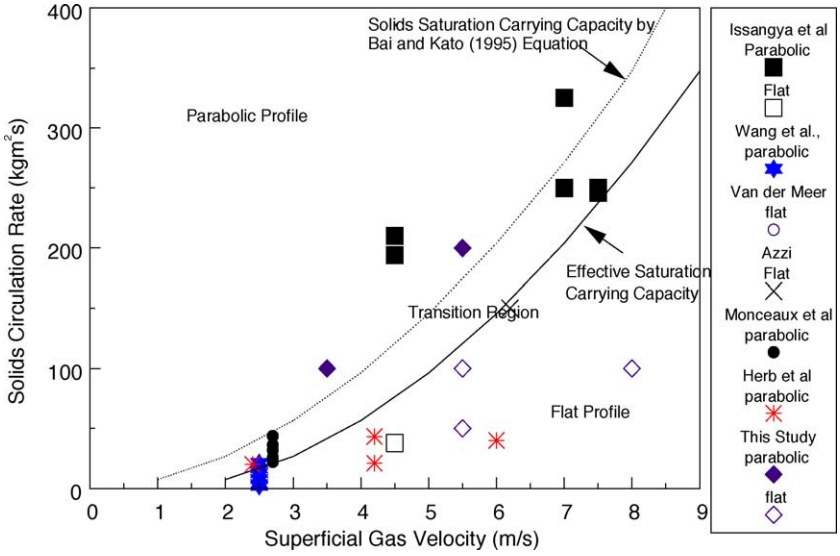

Fig. 6. Division of the two operating regions with parabolic or flat radial solids flux profiles by the effective solids saturation carrying capacity.

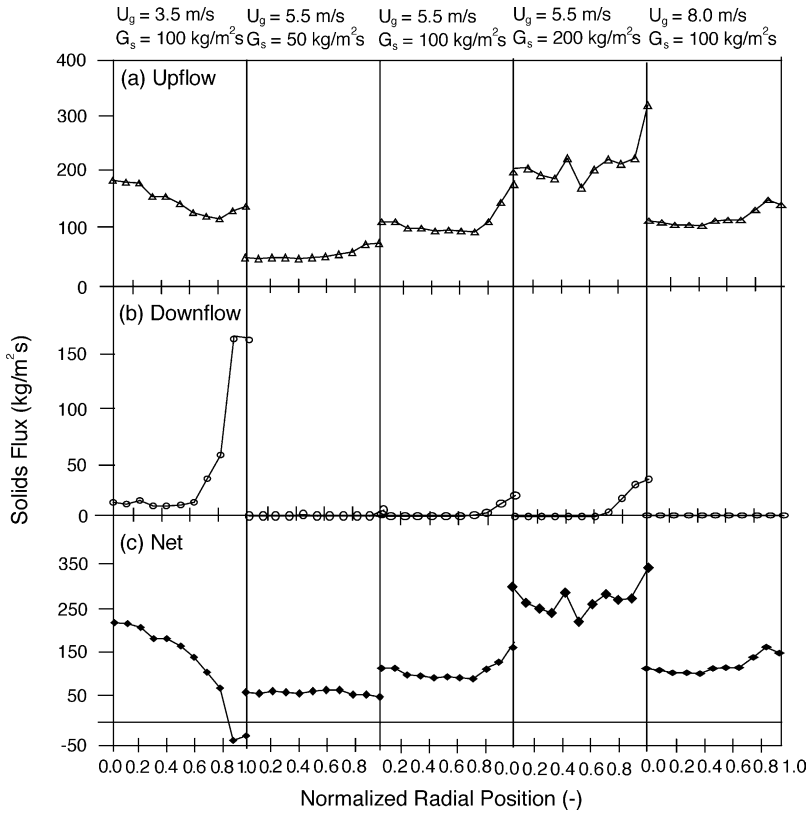

Fig. 7. Effects of operating conditions on the radial profiles of solids flux in the fully developed region (H = 13.67 m) in the 100 mm riser.

bols in Fig. 6 mark the parabolic radial solids flux distribution and the open symbols indicate the more flat profile.

A general trend is clearly seen from this figure: experiments under operating conditions near and above the G_s^* versus U_g curve tend to produce the parabolic shaped radial solids flux distribution and tests under conditions well below the G_s^* versus U_g curve give a much more uniform radial distribution of the solids flux. This is reasonable since the latter conditions (with higher U_g and lower G_s) give the gas more capacity to carry the solids so that solids downflow in the wall region is effectively reduced or eliminated. Above G_s^*, solids cannot be completely carried by the gas so that solids downflow begins to form at the wall, leading to a parabolic shape in the radial solids flux distribution. This seems to indicate that the saturation carrying capacity can be used to roughly divide the two operating regions corresponding to the two different shapes of the radial solids flux profiles.

The fact that the parabolic profile begins to appear at operating conditions somewhat below the G_s^* curve may be explained by the fact that the solids loading in the wall region may have already been over G_s^*, due to the non-uniform radial distribution of solids concentration, even though the overall solids loading is still below G_s^*. Therefore, the boundary, which separates the two operating regions, should be somewhere lower than the saturation capacity curve, as plotted in Fig. 6. These values may be considered as the effective solids saturation carrying capacity. It should also be noted that the

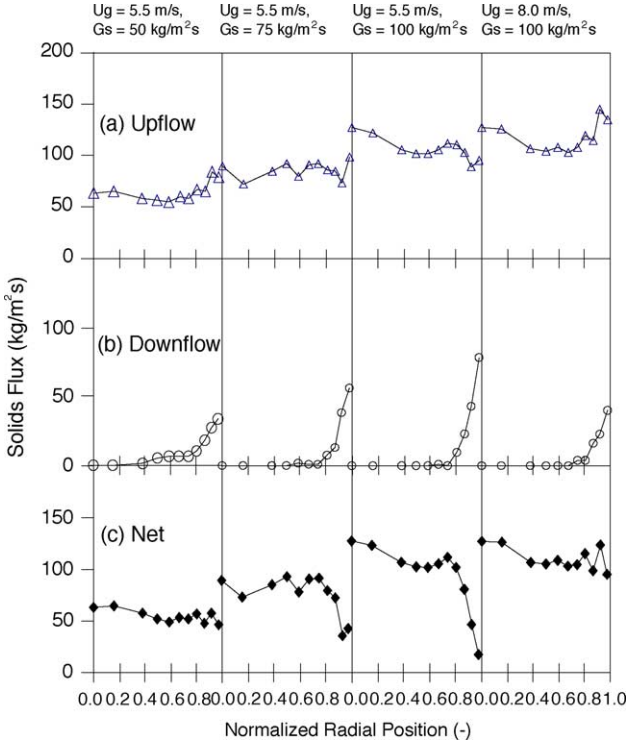

Fig. 8. Effects of operating conditions on the radial profiles of solids flux in the fully developed region (H = 5.84 m) in the 203 mm riser.

results by Herb et al. [11] are not in line with the above postulation, but their data were taken in a very small diameter riser of 5 cm in diameter, where the strong wall effect may have significantly altered the shape of the radial profiles.

Fig. 7 presents results obtained at $H = 13.67$ m in the fully developed region of the 100 mm riser. Fig. 7a presents the data for the upflow solids flux in this riser. Although the shapes of the profiles were not exactly the same as those from the 76 mm column, the general trends are the same. In Fig. 7b, the downflowing solids flux in the 100 mm riser was quite similar to the downflow profiles found in the 76 mm riser as shown in Fig. 5b. The amount of downflowing solids was very small and constant in the central regions of the column and began to increase to a maximum value at the wall. The net solids flux profiles in the 100 mm riser were also found to be similar to those in the 76 mm riser as well. In addition, operating conditions affect the net, upwards and downwards solids flux in the same fashion as those observed in the 76 mm riser. The only obvious exception observed in the 100 mm riser is that the radial profile of solids flux at $G_s = 100$ kg/m^2 s and $U_g = 3.5$ m/s is clearly more parabolic. Fig. 6 suggests that the parabolic shape should be more representative under this operating condition. This will be explained later by comparing the radial profiles of solids flux in different diameter risers.

Fig. 8 presents results obtained at $H = 5.84$ m in the fully developed region of the 203 mm riser. Fig. 8a–c shows the data for the upflow, downflow and net solids flux in this riser. Although the shapes of the profiles were not exactly the same as those from the 76 and 100 mm column, the general trends are the same. In addition, operating conditions affect the net, upwards and downwards solids flux in the same fashion as those observed in the 76 mm riser and 100 mm riser. The only exception is that the radial profile of solids flux at $G_s = 100$ kg/m^2 s and $U_g = 5.5$ m/s in the 203 mm riser is more parabolic. Fig. 6 suggests that this operating condition is on the edge of transition region, and the parabolic shape may appear.

3.2. Development of radial profiles of solids flux

Figs. 9 and 10 show the effect of the axial position on the radial profiles of solids flux. Results obtained in the 76 mm

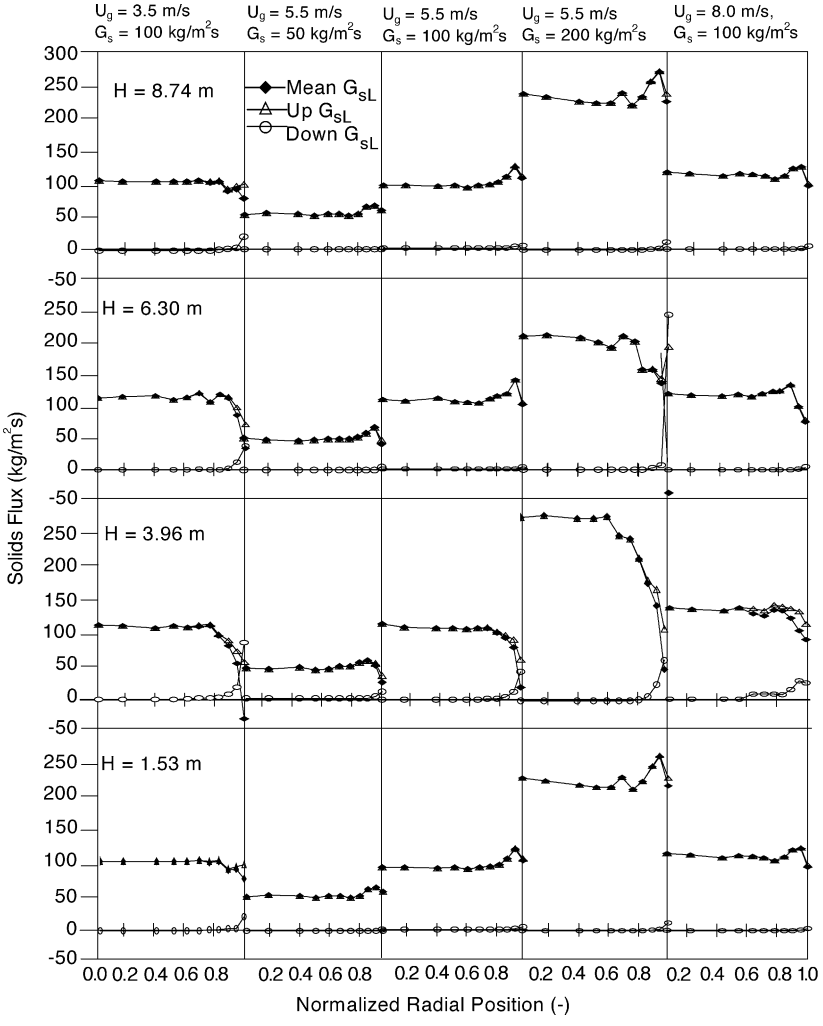

Fig. 9. Effects of axial position and operating conditions on the solids flux in the 76 mm riser.

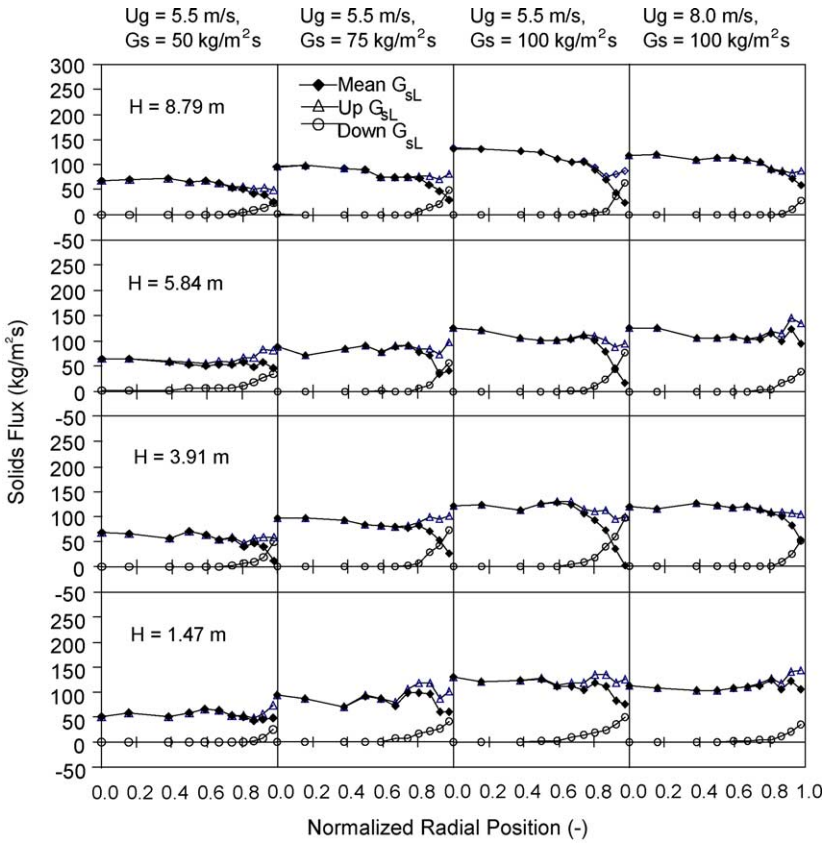

Fig. 10. Effects of axial position and operating conditions on the solids flux in the 203 mm riser.

riser are shown in Fig. 9. The upward G_{sL} was not affected to a large degree by the axial position, but the downward G_{sL} was affected by axial position. For all the conditions studied, increasing the distance from the riser distributor caused decreases in the downflowing solids. This may be attributed to the flow development along the riser column, which is faster in the core, but much slower in the annulus [27]. The amount of downflowing solids was highest in the lower regions of the riser ($H < 4$ m) where the solids acceleration is yet not very significant in the wall region. In the upper regions of the riser ($H = 8.74$ m), the downflowing solids has all but disappeared, accompanied by the fully developed flow in both the core and the annulus. In the very bottom region of the riser ($H = 1.53$ m), there were no downflowing solids. This is probably due to the high levels of initial acceleration that occurs in the riser. Once enter into the system, the particles are rapidly accelerated by the uniformly distributed gas at the riser bottom. As the particles travel up from the distributor, with the gas flow developing into a radial distribution of high velocity in the central and low velocity near the wall, some solids begin to flow downwards near the wall (e.g. at $H = 3.96$ m), where the gas velocity is lower.

Similar tendency was found in the 203 mm riser as shown in Fig. 10. However, in the upper regions of the riser ($H = 8.74$ m), the downflowing solids did not disappear in the 203 mm riser, which indicates the flow development of a larger riser is slower than that of a smaller riser. At the same time, in the very bottom region of the riser ($H = 1.53$ m), there were some downflowing solids. In addition, the downflow G_{sL} at the wall of the 203 mm riser is higher than that of 76 mm riser at all axial levels. That is, particle acceleration at the wall of a larger riser is much slower than that of a smaller riser. Obviously, flow development is slower than with the increase of riser diameter.

Similar tendency was also found in the 100 mm riser. The solids flux data can also be calculated from the measured local particle velocity and solids concentration. Details of the measuring equipment used can be found in [28,29]. A direct comparison between the measured and the calculated solids flux in Fig. 11, at $H = 10.14$ m, shows the good agreement between the two. The profiles obtained at all other axial positions tested in the same riser from the two methods also follow each other quite well. This shows that both methods (direct measurement and calculation from solids velocity and concentration) are acceptable for the measurement of the solids flux. Data in Fig. 9 are from direct measurements in the 76 mm riser.

The shapes of the radial profiles in the 100 mm riser are both parabolic and flat, as was to be expected, according to Fig. 6. At lower values of U_g (3.5 m/s at $G_s = 100$ kg/m^2 s) and higher G_s (200 kg/m^2 s at $U_g = 5.5$ m/s), the shapes of the profiles were parabolic throughout the length of the col-

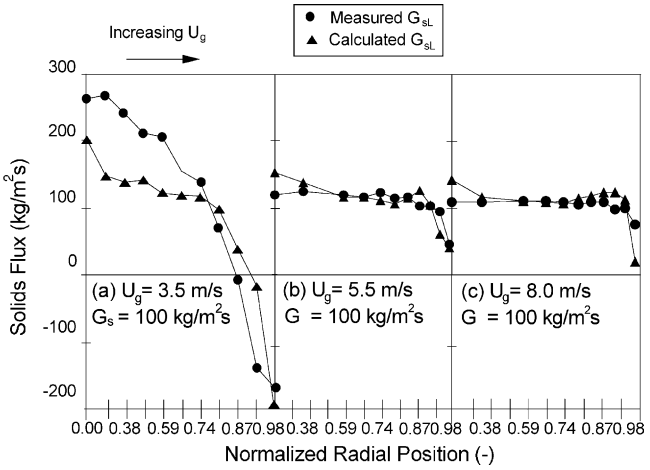

Fig. 11. Comparison between the directly measured solids fluxes, with those calculated from the measured solids velocity and concentration (H = 10.14 m, 100 mm riser).

umn. At the other conditions, the shapes of the profiles were rather flat. The operating conditions affected the shapes of the solids flux profile in the same manner as in the 76 mm riser. Increasing U_g at a constant G_s caused the profiles to become more radially uniform throughout the length of the column, since the increase of U_g reduced the amount of downflowing solids. Increasing G_s caused increases in G_{sL} at every radial position, with the amount of downflowing solids increased as G_s was increased.

When the values of the local solids flux do not change with the axial position, the flow has reached the fully developed point. In Figs. 9–11, the results are quite obvious that increasing U_g will decrease the length of development in the riser. On the other hand, increasing G_s has the same general effect as does decreasing U_g in the risers: the length of development will increase if the G_s is increased at a constant U_g. This is logical as when the solids/air ratio is higher, a larger amount of solids need to be carried by a unit volume of the air so that it will take a longer time for the flow to reach the fully developed point.

3.3. Comparison of radial profiles of solids flux in different diameter risers

Fig. 12 compares the directly measured local net solids fluxes under different operating conditions for three different diameter risers at the fully developed region. It is clearly seen that with the increase of riser diameter, the radial profiles of solids flux become less uniform under different operating conditions. As stated in [30,31], gas encounters much more resistance at the wall than in the centre due to the wall friction, so that, the gas velocity is higher in the centre than that in the wall. With the increase of distance between the wall and the centre under the same superficial gas velocity and solids circulation rate, the difference of gas velocity in these two regions becomes bigger. Thus, in a larger diameter riser, the gas distribution is much less uniform than that in a smaller

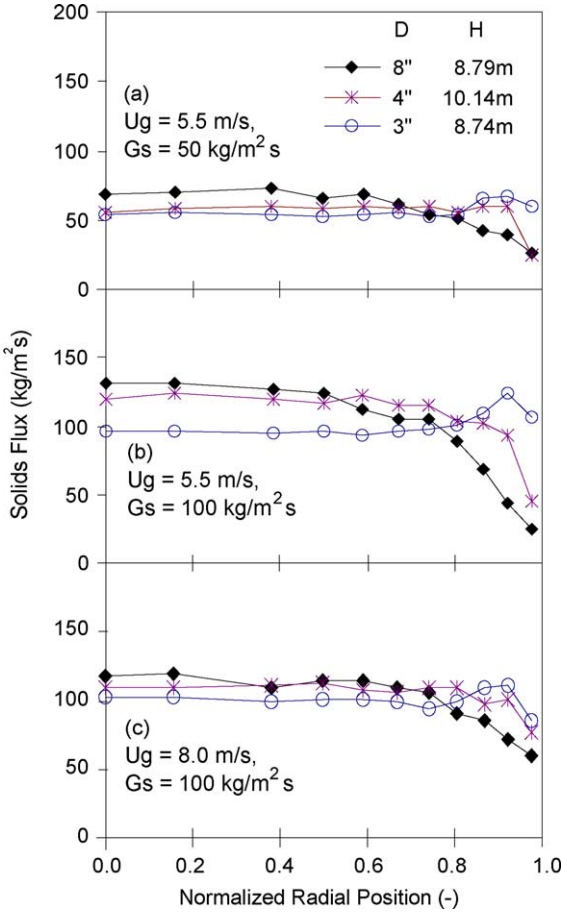

Fig. 12. Comparison of the directly measured local net solids fluxes under different operation conditions for three different diameter risers at the fully developed region.

diameter riser, and the gas velocity of a larger riser is much lower than that of a smaller riser at the wall. As a result, the solids holdup at the wall of a larger riser is higher, which may lead to the solids loading in the wall region higher than G^*, even though the overall loading is still below G^*. At the same time, more particles flow downwards at the wall of the larger riser. This is what has been observed in the current study. As seen in Figs. 9 and 10, the downflow G_{sL} at the wall of the 203 mm riser is higher than that of the 76 mm riser at all axial levels. In addition, the upflow G_{sL} is comparable. Therefore, the net solids flux at the wall of a larger riser is lower than that of a small riser. The radial profile of solids flux is less uniform in a larger riser. This also explains the difference between the radial profiles of solids flux at U_g = 3.5 m/s and G_s = 100 kg/m^2 s, shown in Figs. 5 and 7. It is expected that with an even larger diameter riser (larger than 203 mm), the radial profiles of solids fluxes become less uniform. Further experiments are required to verify it.

4. Conclusions

The following conclusions can be drawn from this study:

Solids flux data determined by direct measurements are in good agreement with those calculated from the measured solids concentration and velocity.

The shapes of the radial solids flux profiles in three risers were found to be either flat with decreasing annulus or parabolic, depending on the operating conditions. The shape of the radial solids flux profile could be predicted using the effective saturation capacity, above which a parabolic profile prevails due to the increased solids downflow near the wall. The radial profile of solids flux is less uniform in a larger riser than in a smaller riser. The amount of downflowing solids is highest in the lower sections of the riser, but then begins to decrease as the measuring point is moved away from the distributor. Increases in U_g cause the amount of downflowing solids at the wall to decrease, resulting in a more flat radial profile of the solids flux in the columns. Increasing G_s increases the amount of downflowing solids, resulting in a more parabolic shape.

The flow development is affected in the same manner in different diameter columns: increases in U_g or decreases in G_s reduce the length of development. Flow development is slower with the increase of riser diameter.

Acknowledgments

The authors would like to acknowledge the National Science and Engineering Research Council of Canada for financial support. Also, the authors greatly appreciate the help provided by X. Zhu, H. Zhang, J. Pärssinen and W.-X. Huang during the experimental phase.

References

[1] E.V. Murphree, C.L. Brown, H.G.M. Fischer, E.J. Gohr, W.J. Sweeney, Fluid Catal. Process., I&EC 35 (1943) 768–773.
[2] J. Yerushalmi, D.H. Turner, A.M. Squires, I&EC, Proc. Des. Dev. 15 (1976) 47–53.
[3] Y. Li, M. Kwauk, Fluidization (1980) 537–544.
[4] E.-U. Hartge, Y. Li, J. Werther, Fluidization V (1986) 345–352.
[5] J. Li, Y. Tung, M. Kwauk, Circulating Fluidized Bed Technol. II (1988) 193–203.
[6] D.-R. Bai, Y. Jin, Z.-Q. Yu, J.-X. Zhu, Powder Technol. 71 (1992) 51–58.
[7] L. Monceaux, M. Azzi, Y. Molodtsof, J.F. Large, Fluidization V (1986) 337–344.
[8] M.J. Rhodes, F. Laussmann, F. Villain, D. Geldart, Circulating Fluidized Bed Technol. II (1988) 155–164.
[9] M. Azzi, P. Turlier, J.F. Large, J.R. Bernard, CFB Technol. II (1991) 189–194.
[10] B.J. Harris, J.F. Davidson, Fluidization VII (1992) 219–226.
[11] B. Herb, S. Dou, K. Tuzla, J. Chen, Powder Technol. 70 (1992) 197–205.
[12] M.J. Rhodes, X.S. Wang, H. Cheng, T. Hirama, Chem. Eng. Sci. 47 (1992) 1635–1643.
[13] M.J. Rhodes, P. Laussmann, Powder Technol. 70 (1992) 141–151.
[14] M. Kruse, J. Werther, Chem. Eng. Process. 34 (1995) 185–203.
[15] W. Nowak, K.K. Win, H. Matsuda, M. Hasatani, M. Kruse, J. Werther, Fluidization VIII (1995) 67–76.
[16] X.S. Wang, B.M. Gibbs, R.J. Rhodes, Fluidized Bed Combustion (1995) 663–670.
[17] E.H. van der Meer, R.B. Thorpe, J.F. Davidson, Circulating Fluidized Bed Technol. V (1996) 575–580.
[18] F. Wei, F. Lu, Y. Jin, Z. Yu, Powder Technol. 91 (1997) 189–195.
[19] A.S. Issangya, D. Bai, J.R. Grace, J. Zhu, Fluidization IX (1998) 197–204.
[20] A.S. Issangya, Ph.D. dissertation, University of British Columbia, 1998.
[21] S.B.R. Karri, T.M. Knowlton, Circulating Fluidized Bed Technol. VI (1999) 71–77.
[22] J.F. Davidson, Powder Technol. 113 (2000) 249–260.
[23] S. Malcus, E. Cruz, C. Rowe, T.S. Pugsley, Powder Technol. 125 (2002) 5–9.
[24] B.J. Harris, Ph.D. dissertation, Cambridge, 1992.
[25] C.C. Werdermann, Ph.D. thesis, Technischen Universitat, 1992, p. 79, 93, 94.
[26] D.-R. Bai, K. Kato, CFB. J. Chem. Eng. Jpn. 28 (1995) 179–185.
[27] D.-R. Bai, J.-X. Zhu, Y. Jin, Z.-Q. Yu, Powder Technol. 85 (1995) 179–188.
[28] H. Zhang, P.M. Johnston, J.-X. Zhu, H.I. de Lasa, M.A. Bergougnou, Powder Technol. 100 (1998) 260–272.
[29] J.-X. Zhu, G.-Z. Li, S.-Z. Qin, F.-Y. Li, H. Zhang, Y.-L. Yang, Powder Technol. 115 (2) (2001) 184–192.
[30] A.-J. Yan, J.-X. Zhu, Ind Eng. Chem. Res. 43 (2004) 5810–5819.
[31] A.-J. Yan, J.-X. Zhu, AIChE, 2005, in press.